Electronic Supplementary Material (ESI) for Journal of Materials Chemistry A.

Supporting Information

Scalable nanomanufacturing of chalcogenide inks: a case study on thermoelectric V–VI nanoplates

Minxiang Zeng,[a] Hongyao Xie,[b] Mortaza Saeidi-Javash,[a] Newaz Mohammad Tanvir,[a] Yipu Du,[a] Jiahao Chen,[a] Mercouri G. Kanatzidis,[b] and Yanliang Zhang[a,*]

[a]*Department of Aerospace and Mechanical Engineering, University of Notre Dame, Notre Dame, IN 46556, USA*

[b]*Department of Chemistry, Northwestern University, Evanston, Illinois 60208, United States*

**Corresponding Authors:* yzhang45@nd.edu.

Table of Contents

Materials characterization

A transmission electron microscope (Titan 80-300) was used to image the samples. A focused ion beam-scanning electron microscope (FIB-SEM, Helios G4 UX) was used to obtain SEM images of samples. A confocal Raman microscope (NRS-5100, Jasco) with high-Speed XYZ imaging capability was used to characterize materials and molecules structure and composition. To map the elemental distribution of combinatorial films, Energy dispersive X-Ray spectroscopy (Helios G4 UX and Titan 80-300) and X-ray fluorescence imaging (EDAX Orbis PC Micro-XRF) were used depending the sample compositions and dimensions.

Densification

The $Bi_2Te_{2.7}Se_{0.3}$ nanoplates were dried at 380 ^oC for 60 min under H_2/Ar airflow, then sintered by spark plasma sintering (SPS) at 480 ^oC under a pressure of 45 MPa in a vacuum for 15 min to obtain fully densified bulk sample with the size of 12.7 mm in diameter and 7 mm in length. The density of the sample achieved was 6.5715 g/cm^3, (theoretical density is 7.77 g/cm^3).

Thermoelectric properties measurements

The sintered samples were cut and polished into two regular shapes with size of $3 \times 3 \times 12$ mm^3 and $6 \times 6 \times 1.5$ mm^3 for electrical properties and thermal conductivity measurement, respectively. The electrical conductivity and the Seebeck coefficient were simultaneously measured under a He atmosphere from 300 to 525 K by the ZEM-3 apparatus (Ulvac Riko, Inc.). The thermal conductivity was determined based on the thermal diffusivity (D) which was measured in an Ar atmosphere by the laser flash diffusivity method (LFA 457; Netzsch), where the heat capacity (C_p) was calculated by the Dulong-Petit law and the sample densities were determined by measuring the mass and dimensions of the sample. The lattice thermal conductivity was obtained by subtracting the electronic thermal conductivity from the measured total thermal conductivity.

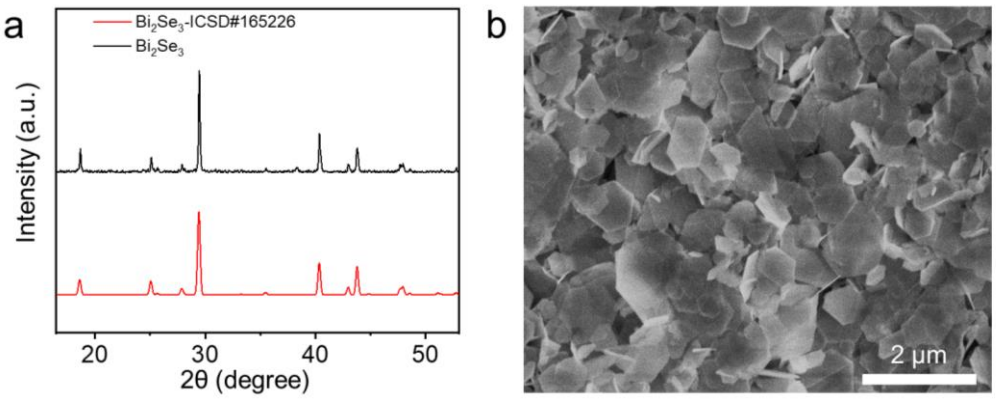

Figure S1. XRD (a) and SEM images (b) of Bi_2Se_3 nanoplates.

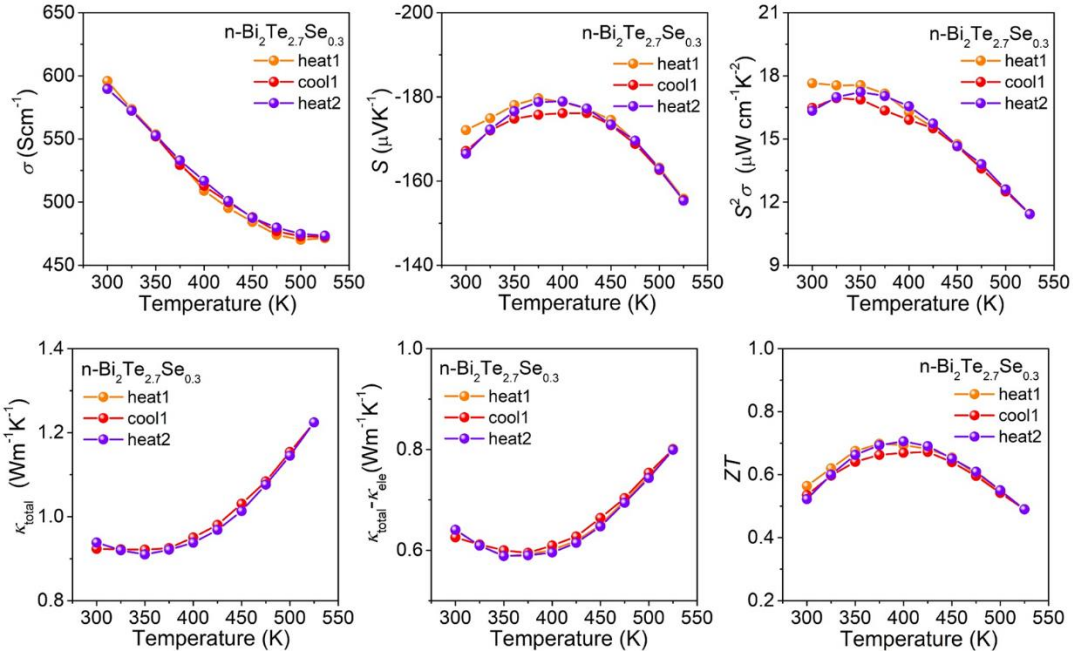

Figure S2. Thermoelectric properties of n-type $Bi_2Te_{2.7}Se_{0.3}$ showing a peak zT of 0.7 at 375-400 K region.

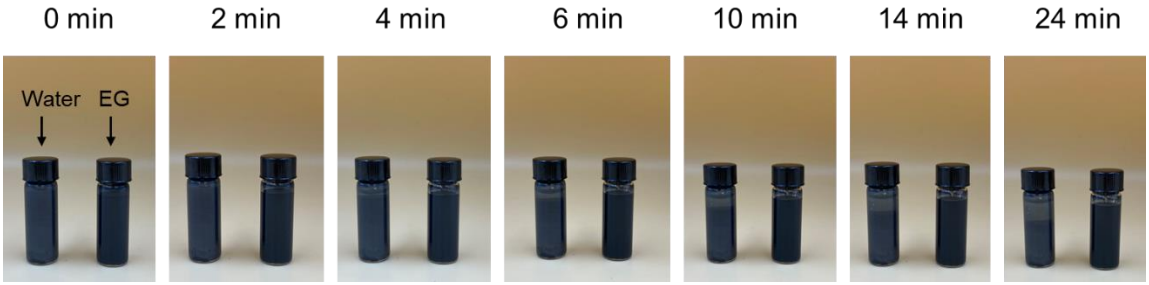

Figure S3. Sedimentation analyses of water-based and EG-based inks ($Bi_2Te_{2.7}Se_{0.3}$ particle concentration: 3.5 wt%).

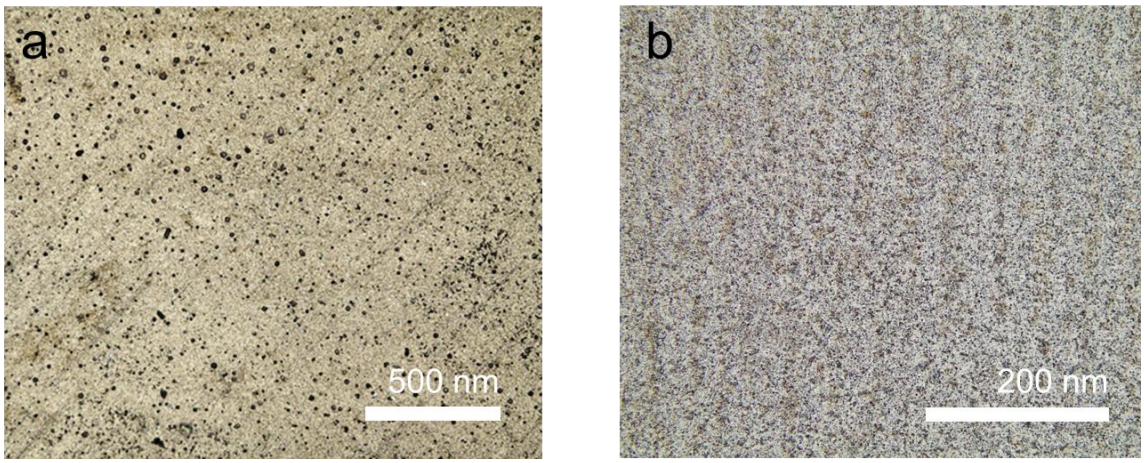

Figure S4. Optical microscopy of printed chalcogenide films using extrusion printing (a) and aerosol jet printing (b) showing no significant coffee-ring effect.

Table S1: Comparison of various synthesis methods under ambient pressure. *Abbreviations: the hydrazine-assisted colloidal synthesis (HCS), ethylene-glycol-assisted colloidal synthesis (ECS), and solvent engineering colloidal synthesis (SCS). Abbreviations of EG and DEG are ethylene glycol and diethylene glycol, respectively.

Method*	**Sb precursor**	**Te precursor**	**Reducing agent**	**Solvent**	**T @ 1 atm**	**Reference**
SCS	$SbCl_3$	Na_2TeO_3	EG	EG/DEG	~191 °C	*This work*
HCS	$SbCl_3$	TeO_2	Hydrazine	EG	~155 °C	[1]
ECS	Sb_2O_3	TeO_2	EG	EG	~180 °C	[2]

Table S2: Comparison of printed thermoelectric materials with processing methods. *The thermal conductivity data are not always readily available for printed TE materials, and thus we here focus on Seebeck coefficient (S), electrical conductivity (σ), and power factor (PF).

Ref.	Materials	Fabrication	Post-treatment	S (μV/K)	σ (S/cm)	PF* μW/(m·K^2)
This work	$Bi_2Te_{2.7}Se_{0.3}$	Extrusion printing	440 °C, 60 min	-172	224	662.9
[3]	$Bi_2Te_{2.8}Se_{0.2}$	Screen printing	430 °C	-126	310	490
[4]	Bi_2Te_3/PEDOT	Screen printing	450 °C	-138	73	138.6
[5]	Bi_2Te_3/epoxy	Extrusion printing	250 °C, 3 h	-157	61	150
[6]	Bi_2S_3/PANI	Drop casting	483 K, 10 min	-42.8	0.4	0.07
[7]	Poly[Kx(Ni-ett)] /PVDF	Inkjet printing	363 K, 10 h	-44.9	2.1	0.4
[8]	V_2O_5/PEDOT	Inkjet printing	100 °C overnight	-350	0.16	2
[9]	Bi_2Te_3/Se/epoxy	Extrusion printing	250/350 °C, 12 h	-170	96	277
[10]	$Bi_2Te_{2.7}Se_{0.3}$	Aerosol jet printing	Photonic sintering, 1.5 s	-163	270	730
[11]	$TiS_2(HA)_x$	Inkjet printing	110 °C	-70	430	211

Table S3. Aerosol jet printing parameters of $Bi_2Te_{2.7}Se_{0.3}$ TE films.

Parameters	Values
Nozzle diameter (μm)	200
Ultrasonic atomizer flow rate (sccm)	28-30
Sheath gas flow rate (sccm)	15-20
Platen temperature (°C)	85
Print speed (mm/s)	4.5

References

(1) Dun, C.; Kuang, W.; Kempf, N.; Saeidi-Javash, M.; Singh, D. J.; Zhang, Y. 3D Printing of Solution-Processable 2D Nanoplates and 1D Nanorods for Flexible Thermoelectrics with Ultrahigh Power Factor at Low-Medium Temperatures. *Advanced Science* **2019,** *6* (23), 1901788.

(2) Zhang, G.; Wang, W.; Lu, X.; Li, X. Solvothermal Synthesis of V−VI Binary and Ternary Hexagonal Platelets: The Oriented Attachment Mechanism. *Crystal Growth & Design* **2009,** *9* (1), 145.

(3) Varghese, T.; Hollar, C.; Richardson, J.; Kempf, N.; Han, C.; Gamarachchi, P.; Estrada, D.; Mehta, R. J.; Zhang, Y. High-performance and flexible thermoelectric films by screen printing solution-processed nanoplate crystals. *Scientific Reports* **2016,** *6*, 33135.

(4) We, J. H.; Kim, S. J.; Cho, B. J. Hybrid composite of screen-printed inorganic thermoelectric film and organic conducting polymer for flexible thermoelectric power generator. *Energy* **2014,** *73*, 506.

(5) Chen, A.; Madan, D.; Wright, P. K.; Evans, J. W. Dispenser-printed planar thick-film thermoelectric energy generators. *Journal of Micromechanics and Microengineering* **2011,** *21* (10), 104006.

(6) Wang, Y.; Liu, G.; Sheng, M.; Yu, C.; Deng, Y. Flexible thermopower generation over broad temperature range by PANI/nanorod hybrid-based p–n couples. *Journal of Materials Chemistry A* **2019,** *7* (4), 1718.

(7) Jiao, F.; Di, C.-a.; Sun, Y.; Sheng, P.; Xu, W.; Zhu, D. Inkjet-printed flexible organic thin-film thermoelectric devices based on p- and n-type poly(metal 1,1,2,2-ethenetetrathiolate)s/polymer composites through ball-milling. *Philosophical Transactions of the Royal Society A: Mathematical, Physical and Engineering Sciences* **2014,** *372* (2013), 20130008.

(8) Ferhat, S.; Domain, C.; Vidal, J.; Noël, D.; Ratier, B.; Lucas, B. Organic thermoelectric devices based on a stable n-type nanocomposite printed on paper. *Sustainable Energy & Fuels* **2018,** *2* (1), 199.

(9) Madan, D.; Wang, Z.; Chen, A.; Juang, R.-c.; Keist, J.; Wright, P. K.; Evans, J. W. Enhanced Performance of Dispenser Printed MA n-type Bi2Te3 Composite Thermoelectric Generators. *ACS applied materials & interfaces* **2012,** *4* (11), 6117.

(10) Saeidi-Javash, M.; Kuang, W.; Dun, C.; Zhang, Y. 3D Conformal Printing and Photonic Sintering of High-Performance Flexible Thermoelectric Films Using 2D Nanoplates. *Advanced Functional Materials* **2019,** *29* (35), 1901930.

(11) Ferhat, S.; Domain, C.; Vidal, J.; Noël, D.; Ratier, B.; Lucas, B. Flexible thermoelectric device based on TiS2(HA)x n-type nanocomposite printed on paper. *Organic Electronics* **2019,** *68*, 256.